Eur. Phys. J. A **16**, 457–467 (2003)
DOI 10.1140/epja/i2002-10130-9

THE EUROPEAN PHYSICAL JOURNAL A

Investigations into the alpha-decay of ^{195}At

H. Kettunen[1,a], T. Enqvist[1], M. Leino[1], K. Eskola[2], P.T. Greenlees[1], K. Helariutta[1,b], P. Jones[1], R. Julin[1], S. Juutinen[1], H. Kankaanpää[1], H. Koivisto[1], P. Kuusiniemi[1], M. Muikku[1,c], P. Nieminen[1], P. Rahkila[1], and J. Uusitalo[1]

[1] Department of Physics, University of Jyväskylä, P.O. Box 35, FIN-40014 Jyväskylä, Finland
[2] Department of Physical Sciences, University of Helsinki, FIN-00014 Helsinki, Finland

Received: 16 September 2002 / Revised version: 4 December 2002 /
Published online: 25 March 2003 –
Communicated by W. Henning

Abstract. The low-energy nuclear structure and decay properties of the neutron-deficient isotopes ^{195}At and ^{191}Bi have been studied. ^{195}At was produced in the reaction ^{142}Nd(^{56}Fe,p2n)^{195}At and ^{191}Bi as the daughter activity of ^{195}At. The activities were implanted in a position-sensitive silicon detector after being separated from the primary beam by a gas-filled recoil separator. The $1/2^+$ intruder state was determined to be the ground state in ^{195}At with an alpha-decay energy of $E_\alpha = 6953(3)$ keV and a half-life $T_{1/2} = 328(20)$ ms. Another state with an alpha-decay energy $E_\alpha = 7075(4)$ keV and a half-life $T_{1/2} = 147(5)$ ms was found to decay to a 148.7(5) keV excited state in ^{191}Bi for which a spin and parity of $7/2^-$ were deduced. Consequently, the same $7/2^-$ character was assigned to the initial state at 32(7) keV in ^{195}At on the basis of unhindered alpha-decay. The $9/2^-$ state, being the ground state in heavier odd-mass astatine isotopes, was not observed.

PACS. 23.60.+e Alpha decay – 27.80.+w $190 \leq A \leq 219$ – 23.20.Lv Gamma transitions and level energies – 21.10.Dr Binding energies and masses

1 Introduction

The first hints for the existence of ^{195}At were deduced in 1967 by W. Treytl and K. Valli [1] who observed its alpha-decay daughter nuclei in an experiment where astatine isotopes from ^{204}At to ^{196}At were produced. Treytl and Valli performed the experiment at the HILAC accelerator in Berkeley using heavy-ion fusion reactions ^{185,187}Re (^{20}Ne, xn)$^{205-x,207-x}$At and the He-jet technique. However, the technique was not fast enough to detect ^{195}At directly.

The synthesis of ^{195}At was first reported in the unpublished works of S. Yashita [2] and M. Leino [3], which were both done employing the gas-filled recoil separator SASSY [4] at the Super-HILAC in Berkeley. The alpha-decay energy and half-life of ^{195}At obtained by Yashita were $E_\alpha = 7120(30)$ keV and $T_{1/2} = 200(100)$ ms, respectively. Leino obtained the same results, but also found an additional alpha-particle transition in ^{195}At with an energy of $E_\alpha = 7190(30)$ keV and a half-life of $T_{1/2} = 140(50)$ ms. In both works, ^{195}At was produced using the heavy-ion fusion reaction ^{141}Pr(^{56}Fe,2n)^{195}At.

The decay properties of ^{195}At have been studied in the unpublished work of T. Enqvist [5], where a complicated decay pattern was observed. It was tentatively concluded that the wide range of ^{195}At alpha-decay energies was due to a contribution of conversion electrons from a low-lying excited state in ^{191}Bi. All or part of the conversion electron energy was summed up with the alpha-decay energy of ^{195}At (pile-up of the signals in the silicon detector). However, the spin and parity of the low-lying level could not be determined with confidence. This experiment was performed at Jyväskylä using the RITU [6] gas-filled recoil separator at the $K = 130$ MeV cyclotron and the ^{141}Pr(^{56}Fe,2n)^{195}At reaction. The alpha-decay energy and half-life of the assumed $1/2^+$ state in ^{195}At were determined to be $E_\alpha = 6953(4)$ keV and $T_{1/2} = (390^{+100}_{-60})$ ms, respectively. For the other transition, after extraction of the contribution of conversion electrons, an alpha-decay energy of $E_\alpha = 7065(10)$ keV and half-life of $T_{1/2} = (142^{+14}_{-12})$ ms were determined. Preliminary results of the work [5] were also reported in ref. [7]

More recently, D. Seweryniak *et al.* [8] claimed the observation of the $1/2^+$ intruder state in ^{195}At decaying

[a] e-mail: heikki.kettunen@phys.jyu.fi
[b] *Present address:* Laboratory of Radiochemistry, P.O. Box 55, FIN-00014, University of Helsinki, Finland.
[c] *Present address:* Radiation and Nuclear Safety Authority, P.O. Box 14, FIN-00881 Helsinki, Finland.

via alpha emission, using the Fragment Mass Analyzer FMA [9] at ATLAS in Argonne to separate reaction products formed in the reaction ^{165}Ho(^{36}Ar,6n)^{195}At. However, no decay energy or half-life values were mentioned.

The latest paper reporting the observation of the alpha-decay energies and half-lives of ^{195}At was published by Y. Tagaya *et al.* [10]. They obtained values of $E_\alpha = 6960(20)$ keV for the alpha-decay energy and $T_{1/2} = (385^{+69}_{-51})$ ms for the half-life of an isomeric state in ^{195}At. For the ground-state decay they measured $E_\alpha = 7105(30)$ keV and $T_{1/2} = (146^{+21}_{-17})$ ms. The experiment was carried out using the gas-filled recoil separator GARIS [11] at the RIKEN Accelerator Research Facility (RARF). A spin and parity of $(1/2^+)$ were assigned to the isomeric state in ^{195}At by Tagaya *et al.* [10].

In the experiments performed at Argonne [8] and RIKEN [10], evaporation residues were implanted in a position-sensitive silicon-strip detector. The identification of the implanted recoiling nuclei was based on time- and position-correlated alpha-decay chains.

Odd-Z, even-N nuclei in the vicinity of the $Z = 82$ shell closure provide excellent opportunities for investigating the phenomenon of shape coexistence at low excitation energies. In light neutron-deficient, even-N gold ($Z = 79$) and thallium ($Z = 81$) nuclei below the $Z = 82$ shell closure, low-lying $9/2^-$ states have been identified in alpha-decay measurements. These intruder states with $\pi(1p - 4h)$ and $\pi(1p - 2h)$ configurations result from proton excitations across the $Z = 82$ shell gap to the $\pi h_{9/2}$ orbital and are associated with an oblate-deformed shape coexisting with the near-spherical $1/2^+$ ($\pi s_{1/2}$) state (ground state in thallium isotopes) [12,13]. In odd-mass bismuth ($Z = 83$) nuclei above the $Z = 82$ shell closure, the intruder states have been identified as $s_{1/2}$ proton hole states ($\pi(2p - 1h)$ configuration) and the ground states as $\pi h_{9/2}$ particle states [13,14].

The first identification of a $1/2^+$ intruder state in astatine ($Z = 85$) isotopes was reported by Coenen *et al.* [15] and the state was assigned to ^{197}At. The low excitation energy (52 keV) of the intruder state in ^{197}At led them to the conclusion, that the $1/2^+$ state may become the ground state in ^{195}At.

The excitation energies of the $9/2^-$ intruder states in odd-mass thallium isotopes exhibit a parabolic behaviour as a function of neutron number having the minimum close to the mid-shell at $N = 108$ [12,13]. A similar parabolic energy dependence on neutron number has also been observed for the $1/2^+$ intruder state in the odd-mass bismuth isotopes. However, as shown by Batchelder *et al.* [14], the excitation energy of the $1/2^+$ intruder state is still decreasing at the $N = 104$ mid-shell nucleus ^{187}Bi. In ref. [14] it was speculated that the continuing downward trend could arise from a crossing of two different $1/2^+$ states. A weakly oblate-deformed intruder state with $\pi(2p - 1h)$ configuration would create the parabolic behaviour in the heavier odd-mass bismuth isotopes. In the lighter isotopes a prolate $1/2^+$ state, associated with a prolate $1/2^+[660]$ Nilsson orbital [14], would cross the oblate state and continue the downward trend of the $1/2^+$ state. The assumption was based on the coexistence of oblate, prolate and also spherical shapes observed in lead isotopes [16].

The observation of proton and alpha-particle emissions from the $1/2^+$ intruder state in ^{185}Bi [17,18] could not establish the excitation energy of that state since no decays from the $9/2^-$ state were seen, which was particularly surprising as remarked by Poli *et al.* [18]. Also, it has been speculated that the $1/2^+$ intruder state would become the ground state in ^{185}Bi.

2 Experiment

In the present work, a heavy-ion–induced fusion-evaporation reaction with ^{56}Fe^{11+} ion beam impinging on a ^{142}Nd target was used. The ^{195}At isotope was produced via the p2n-channel, as a side-product in the study of ^{195}Rn discussed in ref. [19].

Two sets of ^{142}Nd targets, one being a single 500 μg/cm^2 thick foil and the other a stack of two 500 μg/cm^2 thick foils, with an enrichment of 98.26% were used. The foils were prepared by rolling and the percentages of the other neodymium isotopes in the material were: 0.71%, 0.58%, 0.12%, 0.24% for ^{143}Nd to ^{146}Nd, 0.05% for ^{148}Nd and 0.04% for ^{150}Nd.

The ^{56}Fe beam was produced by the MIVOC method [20] in the ECR ion source and was delivered to the target by the $K = 130$ MeV cyclotron of the Accelerator Laboratory at the Department of Physics of the University of Jyväskylä (JYFL). The primary-beam intensities varied between 20 pnA and 30 pnA measured in a Faraday cup in front of the carbon beam window of the gas-filled separator. The total beam on target time was 136 hours.

Five bombarding energies, varying from 255 MeV to 268 MeV in the middle of the ^{142}Nd target were used. The energies were adjusted by using a set of nickel and carbon foils in front of the target to degrade the 275 MeV ^{56}Fe primary-beam energy. Energy losses in the degrader foils, beam window, target and also in the helium filling-gas of the separator were calculated using the TRIM code [21].

The gas-filled recoil separator RITU was used to separate evaporation residues formed in fusion reactions from the primary beam and to transport them to the focal plane. The evaporation residues were implanted into a 305 μm thick position-sensitive silicon detector with dimensions of 80 mm in the horizontal and 35 mm in the vertical direction. The silicon detector was horizontally divided into 16 position-sensitive strips with a vertical position resolution better than 500 μm in each strip.

A multiwire proportional avalanche gas counter was placed 100 mm in front of the silicon detector in order to discriminate alpha-particle decays in the silicon detector from the implantations of scattered beam particles and low-energy evaporation residues. It also allowed separation of the candidate fusion-evaporation residues from the scattered beam particles by combining the energy loss signal in the gas counter with the implantation energy signal in the silicon detector.

The pressure of the helium filling-gas in RITU was typically 1.0 mbar and the gas volume was separated from the high vacuum of the cyclotron beam line by a 50 μg/cm^2 carbon foil. The gas counter was filled with isobutane at a pressure of 3.0 mbar and enclosed by two 120 μg/cm^2 mylar foils from the helium filling-gas of the separator and the silicon detector high-vacuum chamber. The silicon detector was cooled to 253 K using circulating coolant.

In order to detect gamma-ray events at the focal plane in prompt coincidence with alpha-decays, a single Nordball-type (40% relative efficiency) Compton-suppressed germanium detector was placed adjacent to the silicon detector.

Evaporation residues implanted into the silicon detector were identified by the method of time and position correlated decay chains of the type ER $-\ \alpha_{\rm m} - \alpha_{\rm d}$ [22,23], where ER stands for the evaporation residue, $\alpha_{\rm m}$ for the mother and $\alpha_{\rm d}$ for the daughter alpha-particle. The size of the position windows between ER $-\ \alpha_{\rm m}$ and $\alpha_{\rm m} - \alpha_{\rm d}$ pairs were chosen according to the position resolution. The maximum search time for $\alpha_{\rm m}$ and $\alpha_{\rm d}$ was limited either by the half-life of the activity in question or the counting rate in the silicon detector.

The alpha-decay energies observed in the silicon detector were calibrated using well-known alpha activities produced during the experiment and in the bombardment of a ^{106}Cd target by the ^{56}Fe ion beam. The ^{106}Cd target was used to produce known alpha activities with high alpha-decay energies and sufficient yields. The alpha-active nuclei and the corresponding alpha-decay energies used for the energy calibration are presented in table 1. The alpha-decay energy resolution (full width at half-maximum) after summing up all the 16 strips was measured to be about 25 keV at an alpha-decay energy of 7000 keV.

Table 1. Activities used for alpha-decay energy calibration.

Nucleus	Alpha-decay energy (keV)	Reference
^{151}Ho	4521(5)	[24]
^{172}Os	5106(10)	[24]
^{155}Yb	5202(4)	[24]
^{158}Hf	5269(4)	[24]
^{154}Yb	5331(4)	[24]
^{155}Lu	5655(5)	[24]
^{157}Hf	5729(4)	[24]
^{158}Ta	6046(4)	[24]
^{155}Lu	7390(5)	[24]
^{156}Hf	7782(4)	[24]
^{191}Bi	6311(5)	[13]
^{196}Po	6521(5)	[25]
^{195g}Po	6606(5)	[25]
^{195m}Po	6699(5)	[25]
^{194}Po	6842(6)	[25]
^{192}Po	7167(7)	[25]
^{197}At	6958(5)	[26]
^{196}At	7055(7)	[1]

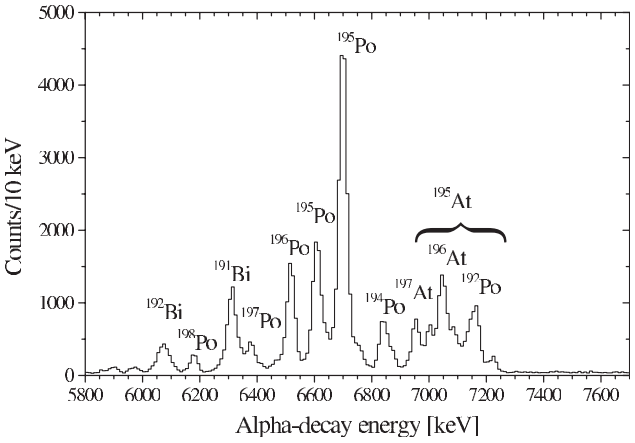

Fig. 1. Energy spectrum of alpha-decays from the reaction ^{56}Fe + ^{142}Nd measured in the silicon detector and vetoed with the gas counter.

3 Data analysis and results

The alpha-decay energy spectrum observed in the present work from the reaction ^{56}Fe + ^{142}Nd is shown in fig. 1. The spectrum was collected in the focal-plane silicon detector and vetoed with the gas counter to suppress the scattered beam particles. Some of the evaporation residues (for example, ^{197,198}Po and ^{197}At) were produced in reactions with heavier neodymium isotopes which comprise 1.74% of the target.

The data analysis was based on the search for correlated decay chains. Low-energy escape alpha-particles which leave the detector and only deposit part of their energy in the silicon were not searched for. The requirement that all events in the chain are recorded within a given position window and within pre-determined time intervals had to be fulfilled.

The alpha-decay energies for correlated decay chains of the type ER $-\ \alpha_{\rm m} - \alpha_{\rm d}$ are shown in fig. 2. The maximum search times used were 1.5 s for ER $-\ \alpha_{\rm m}$ and 80 s for $\alpha_{\rm m} - \alpha_{\rm d}$ correlations. Various search times were used when different groups in fig. 2 were studied in more detail (see table 2). The full width of the position window was approximately 500 μm in the vertical direction.

Two groups of correlated decay chains are clearly observed in fig. 2 when the daughter alpha-decay energy is below 6200 keV. The group with an alpha-decay energy of $E_\alpha = 7166(8)$ keV and half-life $T_{1/2} = 37(4)$ ms for the mother activity and $E_\alpha = 5970(8)$ keV and $T_{1/2} = 26(3)$ s for the daughter activity was determined to originate from the decay chain starting from ^{192}Po. The group with an alpha-decay energy of $E_\alpha = 7048(6)$ keV and half-life $T_{1/2} = 310(40)$ ms for the mother activity and $E_\alpha = 6062(6)$ keV and $T_{1/2} = 47(10)$ s for the daughter activity was determined to originate from the decay chain starting from ^{196}At. The results obtained are compatible with the previously measured values $E_\alpha = 7167(7)$ keV and $T_{1/2} = 34(3)$ ms for ^{192}Po [25], and $E_\alpha = 7055(7)$ keV and $T_{1/2} = 253(9)$ ms for ^{196}At [1,27]. The alpha-decay chains originated from the decay of ^{195}Rn [19] are also

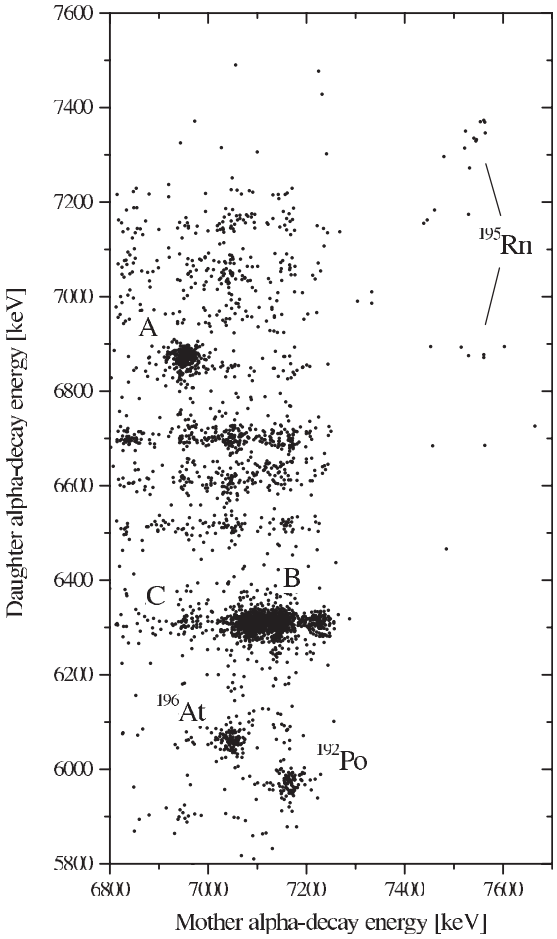

Fig. 2. Two-dimensional display of mother and daughter alpha-decay energies for all correlated decay chains of the type ER$-\alpha_{\rm m}-\alpha_{\rm d}$ observed in the reaction ^{56}Fe + ^{142}Nd. Maximum search times were 1.5 s for the ER $-\ \alpha_{\rm m}$ pairs and 80 s for the $\alpha_{\rm m}-\alpha_{\rm d}$ pairs. The results obtained for ^{195}Rn are discussed in ref. [19].

shown in fig. 2 to give a better idea about the overall background of ER $-\ \alpha_{\rm m}-\alpha_{\rm d}$ correlated decay chains.

3.1 Alpha-decay of the $1/2^+$ state in ^{195}At

An alpha-decay energy of $E_\alpha = 6870(3)$ keV and half-life $T_{1/2} = (121^{+8}_{-7})$ ms were determined from 270 correlated decay chains for the daughter activity of group A in fig. 2. This activity was assigned to the alpha-decay of the $1/2^+$ isomeric state in ^{191}Bi. The results are compatible with the previously reported values of $E_\alpha = 6876(5)$ keV and $T_{1/2} = 150(15)$ ms [13] for the decay of the $1/2^+$ isomeric state in ^{191}Bi. For the mother activity an alpha-decay energy of $E_\alpha = 6953(3)$ keV and half-life $T_{1/2} = 328(20)$ ms were measured. This activity was assigned to originate from the corresponding $1/2^+$ state in ^{195}At due to the unhindered alpha-decay with hindrance factor of 0.92(7) (see table 3) determined according to the method of Rasmussen [28]. The maximum search times used for ER$-\alpha_{\rm m}$ and $\alpha_{\rm m}-\alpha_{\rm d}$ correlation pairs were both 4 s.

Table 2. The numbers of observed ER $-\ \alpha_{\rm m}-\alpha_{\rm d}$ correlated decay chains ($N_{\rm obs.}$) and maximum search times used in correlation of ER $-\ \alpha_{\rm m}$ and $\alpha_{\rm m}-\alpha_{\rm d}$ pairs of different groups in fig. 2. $N_{\rm acc}^{\rm triple}$ represents the expected number of accidentally correlated triple chains, where both correlations ER $-\ \alpha_{\rm m}$ and $\alpha_{\rm m}-\alpha_{\rm d}$ are random. $N_{\rm acc}^{{\rm ER}\alpha_{\rm m}-\alpha_{\rm d}}$ represents the expected number of accidental correlations between the observed ER $-\ \alpha_{\rm m}$ pairs and candidate daughter alpha-decays. The estimates were calculated according to ref. [22].

Group	Search times		$N_{\rm obs.}$	$N_{\rm acc}^{\rm triple}$	$N_{\rm acc}^{{\rm ER}\alpha_{\rm m}-\alpha_{\rm d}}$
	ER $-\ \alpha_{\rm m}$	$\alpha_{\rm m}-\alpha_{\rm d}$			
A	4 s	4 s	270	0.2	0.6
B	1.5 s	80 s	1200	2.9	59
C	4 s	80 s	63	0.8	17

The number of correlated triple chains of the type ER $-\ \alpha_{\rm m}-\alpha_{\rm d}$ produced by random correlations in the energy region of 6900 keV–7000 keV for mother and 6800 keV–6900 keV for daughter alpha-decay was estimated to be 0.2. Correspondingly, the number of random correlations between the found ER $-\ \alpha_{\rm m}$ correlation pairs and candidate daughter alpha-decays was estimated to be 0.6. The estimations of random correlations (presented in table 2) were determined according to ref. [22].

3.2 Alpha-decay of the $7/2^-$ state in ^{195}At

The interpretation of the wide group marked by B in fig. 2 is more complicated. The structure in the alpha-decay energy spectrum of the corresponding mother activities is more evident in fig. 3a as a solid line. Peaks around 7085 keV, 7140 keV and 7220 keV stand out in the spectrum. The similarity in the properties of the corresponding daughter activities ($E_\alpha = 6308(3)$ keV and $T_{1/2} = 12.4(6)$ s, $E_\alpha = 6308(3)$ keV and $T_{1/2} = 11.7(6)$ s and $E_\alpha = 6309(4)$ keV and $T_{1/2} = 13.3(12)$ s, respectively) leads to the conclusion that all three daughter activities originate from the decay of the same initial state. The obtained values of $E_\alpha = 6308(3)$ keV and $T_{1/2} = 12.4(4)$ s for the daughter alpha-decay determined from the combined data including 1200 ER $-\ \alpha_{\rm m}-\alpha_{\rm d}$ correlated decay chains are in good agreement with the previously measured values of $E_\alpha = 6311(5)$ keV and $T_{1/2} = 12(1)$ s for the $9/2^-$ ground-state alpha-decay in ^{191}Bi [13]. The maximum search times used in the analysis were 1.5 s and 80 s for mother and daughter alpha-decays, respectively.

Based on coincident gamma-ray events observed in the germanium detector, it was concluded that the complicated structure in the mother alpha-decay energy spectrum shown in fig. 3a can be explained by the effect of the summing up of the conversion electron energies with the alpha-decay energies. A two-dimensional display of the gamma-ray energy observed in the focal-plane germanium detector within a ~ 20 ns time interval after the observation of the corresponding alpha-decay energy in the silicon

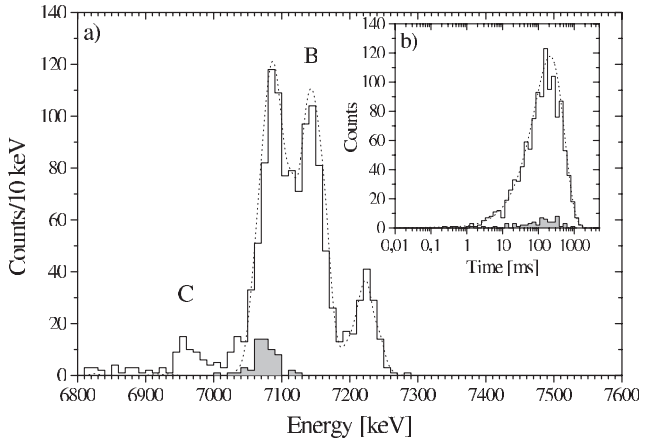

Fig. 3. a) Mother alpha-decay energy spectrum extracted from ER $-$ $\alpha_{\rm m}$ $-$ $\alpha_{\rm d}$ correlated decay chains with daughter alpha-decay energies in the range 6250 keV–6350 keV (solid line). The result of a Monte Carlo simulation is plotted as a dotted line. The filled area represents the energy spectrum of alpha-decays detected in coincidence with 148.7(5) keV gamma-ray events (see figs. 4 and 5) and correlated with evaporation residues. b) The solid line represents the observed time distribution of the mother alpha-decay times in the ER $-$ $\alpha_{\rm m}$ $-$ $\alpha_{\rm d}$ correlated decay chains of the group marked by B. (The same chains as in a), but for mother alpha-decay energies $E_\alpha > 7000$ keV.) The dotted line represents the density distribution of decay times in a radioactive decay [22]. The position of the distribution comes from the experimentally determined half-life $T_{1/2} =$ 147 ms. The filled spectrum represents the time distribution of mother alpha-decays detected in coincidence with 148.7(5) keV gamma-ray events and correlated with evaporation residues.

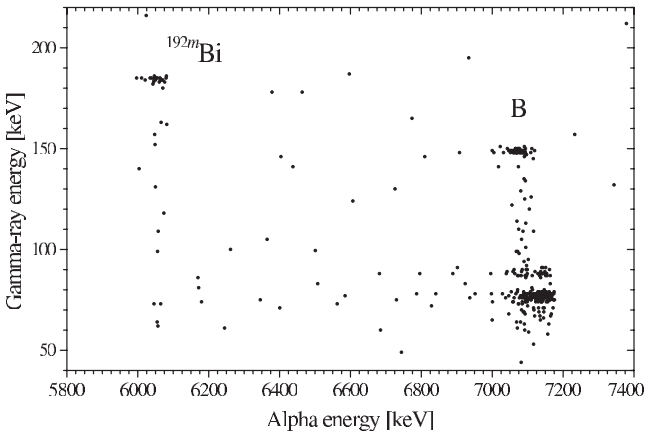

Fig. 4. Two-dimensional display of energies of coincident gamma-ray events and alpha-decays in the reaction ^{56}Fe + ^{142}Nd.

detector is shown in fig. 4. One cluster of previously known alpha-gamma coincidence pairs with $E_\alpha = 6060$ keV and $E_\gamma = 185$ keV was clearly observed and identified as the alpha decay of ^{192m}Bi to the excited state at 184.6 keV in ^{188m}Tl, decaying by a gamma-ray transition to the ground state [29,30].

Figure 5a shows a low-energy part of the gamma-ray energy spectrum where the gamma-ray events were observed within a 8 μs time coincidence with any event in the silicon detector. The gamma-ray energy spectrum for the prompt ($\sim$ 20 ns) alpha-gamma coincidence pairs with the alpha-decay energy greater than 7000 keV is shown in fig. 5b. In total 66 gamma-ray events with an energy of $E_\gamma = 148.7(5)$ keV were observed in prompt coincidence ($T_{1/2} < 10$ ns) with the alpha-particles; 57 of the alpha-particles in the coincidence pairs were correlated with an evaporation residue with $E_\alpha = 7074(4)$ keV and $T_{1/2} = (125^{+20}_{-15})$ ms. The energy spectrum of the correlated alpha-decays is shown in fig. 3a as a filled spectrum. In addition, 18 of the correlated coincidence pairs were correlated with a subsequent daughter alpha-decay with $E_\alpha = 6309(6)$ keV and $T_{1/2} = 7(3)$ s.

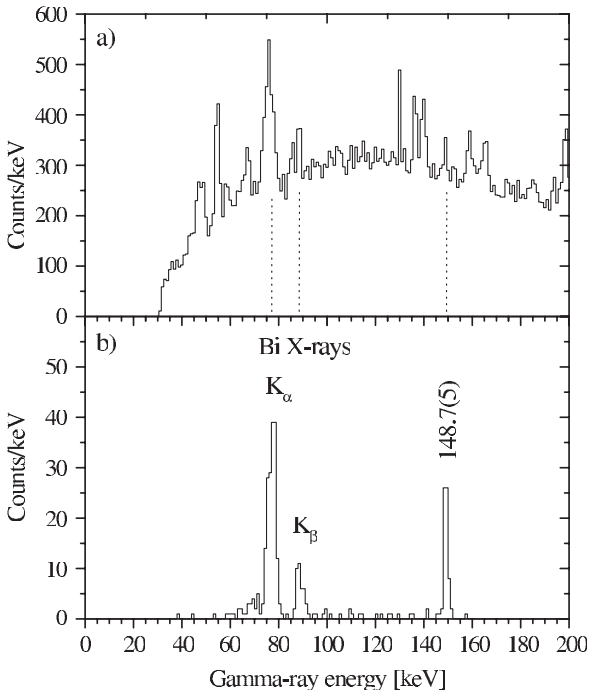

Fig. 5. a) A part of the energy spectrum for gamma-ray events observed in coincidence within a 8 μs time interval with any event in the silicon detector. b) Energy spectrum of gamma-rays in prompt coincidence with alpha-decays of energy greater than 7000 keV in fig. 4.

The other two peaks in fig. 5b correspond to bismuth K X-rays. When X-rays were also allowed to coincide with mother alpha-particles in total 250 ER $-$ $\alpha_{\rm m}$ correlated decay chains were observed with alpha-decay half-life of $T_{1/2} = 145(10)$ ms. In addition, 68 of these were correlated with a subsequent alpha-decay with $E_\alpha = 6309(4)$ keV and $T_{1/2} = (10.5^{+1.4}_{-1.1})$ s for the daughter activity. It was concluded that the X-rays originate from the internal K conversion of the $E = 148.7(5)$ keV transition after the parent alpha-decay.

The numbers of ER $-$ $\alpha_{\rm m}$ and ER $-$ $\alpha_{\rm m}$ $-$ $\alpha_{\rm d}$ correlated decay chains where the mother alpha-particle is in coincidence with an event in the germanium detector allow an estimation of the absolute alpha-decay branching ratio of the $9/2^-$ state in the daughter nucleus ^{191}Bi. The

requirement of coincidences ensures that especially the ER $-$ $\alpha_{\rm m}$ correlations originate from the alpha-decay of ^{195}At. A branching ratio of 59(14)% was obtained when coincidences only with E_γ = 148.7(5) keV gamma-rays were demanded. When bismuth X-rays, in addition to the gamma-rays, were also allowed to coincide with mother alpha-decays, an absolute alpha-decay branching ratio of 51(10)% was obtained for the decay of the $9/2^-$ state in the daughter nucleus ^{191}Bi. In the calculation, a 55% probability that the alpha-particle deposits all its kinetic energy in the silicon detector and 97% relative alpha-decay branching ratio from the $9/2^-$ ground state in ^{191}Bi to the $9/2^-$ state in ^{187}Tl were assumed [13,30].

The difference between the two obtained alpha-decay branching ratio values is most probably just due to statistical variation. Another possibility is that the X-ray peaks were affected by alpha–X-ray coincidences originating from another bismuth isotope. Especially the value determined using only the K_α X-ray peak in fig. 5b is a little lower than values determined using the gamma or K_β X-ray peaks. Even though there is a significant background below the bismuth K_α X-ray in fig. 5a, no significant background could be observed in the two-dimensional alpha-gamma coincidence display in fig. 4. Thus, the absolute alpha-decay branching ratio of the $9/2^-$ state in ^{191}Bi was deduced to be 51(10)% based on the data where the mother alpha-decays were observed in coincidence with E_γ = 148.7(5) keV gamma-rays or bismuth X-rays. The result is compatible with the previously measured value of (44–70)% reported in ref. [13].

The observed gamma-ray energy of E_γ = 148.7(5) keV and half-life $T_{1/2} < 10$ ns limit the possible multipolarity of the transition to $E1$, $M1$ or $E2$. The Weisskopf estimates for a 150 keV transition in bismuth corrected for internal conversion taken from ref. [31] are: $T_{1/2}(E1) = 50$ fs, $T_{1/2}(M1) = 1.5$ ps, $T_{1/2}(E2) = 50$ ns and $T_{1/2}(M2) = 600$ ns.

The K conversion coefficient of the transition can be determined from the intensity ratio of the gamma-ray and K X-rays after corrections for the germanium detector efficiency. The conversion coefficient was determined for the events in coincidence with alpha-decays with an energy greater than 7000 keV (see fig. 5b) and correlated with evaporation residues. The coefficient was also determined for the events with an additional requirement of subsequent daughter alpha-decay in the region of group B in fig. 2. This was done to be sure that possible background in the X-ray peaks did not significantly affect the result. The obtained value $\alpha_K = 3.3(3)$ is in good agreement with the conversion coefficient for an $M1$ transition with α_K = 2.85 given in ref. [31]. The conversion coefficients for the other possible transitions $\alpha_K(E1) = 0.13$, $\alpha_K(E2) = 0.31$ and $\alpha_K(M2) = 13.8$ differ clearly from the value measured in the present work.

The alpha-decay energy for the ^{195}At decay to the excited state in ^{191}Bi was determined from the 57 ER $-$ $\alpha_{\rm m}$ correlated alpha-particles in coincidence with 148.7(5) keV gamma-rays. The energy spectrum of the corresponding alpha-decays is shown in fig. 3a as a filled spectrum. The coincidences with the full-energy gamma-ray events ensure that no additional energy from conversion electron or X-ray cascades were summed up to the alpha-decay energy. The alpha-decay energy directly to the ground state in ^{191}Bi was determined from the alpha peak above 7175 keV shown in fig. 3a. This peak represents both the energy of the direct alpha-decays to the ground state and the alpha-decays to the excited state fully summed up with the energy emitted in the electron conversion (mainly from L and M electron shells) and the following X-ray cascade. More detailed consideration about the summing process and the origin of the various peaks in fig. 3a is given further on in this section. The final results E_α = 7075(4) keV for the alpha-decay energy to the excited state and E_α = 7221(4) keV to the ground state were determined by taking into account the 148.7(5) keV energy difference between the final states in ^{191}Bi. The corresponding half-life $T_{1/2}$ = 147(5) ms of the mother activity was determined from 1200 ER $-$ $\alpha_{\rm m}$ $-$ $\alpha_{\rm d}$ correlated decay chains in group B shown in figs. 2 and 3a. The corresponding time distribution of the mother alpha-decays is shown in fig. 3b as a solid line. The dotted line represents the density distribution of decay times in a radioactive decay [22] when a half-life of $T_{1/2}$ = 147 ms is assumed.

In order to study the summing effect of the conversion electron energies with alpha-decay energies in a silicon detector in more detail, a Monte Carlo simulation program was developed [32]. In the simulation, the realistic physical environment was taken into account by including, for example, the following ingredients in the program: the implantation depth distribution of the evaporation residues in the silicon detector, the detector energy resolution, the alpha-decay energy to the final states, the gamma-ray transition energy from the excited state to the ground state in the daughter nucleus and the relative branching ratios of the alpha-decay to the ground and excited states. The internal conversion coefficients, X-ray energies and intensities and electron binding energies needed for the simulation were taken from ref. [30].

The alpha-decay energy spectrum obtained from the Monte Carlo simulation is shown in fig. 3a as a dotted line. In the simulation, alpha-decay branching ratios of 95.5% and 4.5% from ^{195}At to the 148.7(5) keV excited state and $9/2^+$ ground state in ^{191}Bi, respectively, were assumed. The alpha-decay branching ratios were deduced using the simulation program. An $M1$ multipolarity was assumed for the 148.7(5) keV transition in ^{191}Bi. The simulated spectrum is in good agreement with the measured spectrum plotted by the solid line. No satisfactory agreement with the measured spectrum could be achieved if any other multipolarity than $M1$ for the gamma-ray transition or different alpha-decay branching ratios were assumed.

On the basis of the simulation, the structure in the mother alpha-decay energy spectrum shown in fig. 3a is well understood. The peak around 7085 keV represents the alpha-decay of ^{195}At to the excited state in ^{191}Bi. The shift of approximately 10 keV compared to the value determined from the alpha-gamma coincidences (see the filled spectrum in fig. 3a) is caused by summing the alpha-decay

energy with the energy deposited by the escaped conversion electron in silicon detector before leaving the detector and the following low-energy (< 20 keV) X-ray cascade. The 7140 keV alpha peak can be explained by summing the alpha-decay energy with the K conversion electron energy and the following low-energy X-ray cascade. About 45% of the counts in the 7221(4) keV alpha peak in fig. 3a can be explained as being due to the 4.5% branching ratio to the ground state in ^{191}Bi. The remaining (55%) of the counts can be explained by summing the energy of the alpha-decay to the excited state with the L or M conversion electron kinetic energy and with the energy of the following low-energy X-ray cascade.

Based on the half-life, the K conversion coefficient and the result of the simulation, it was concluded that the gamma-ray transition from the 148.7(5) keV excited state to the $9/2^-$ ground state in ^{191}Bi is of $M1$ character. Therefore, the excited state has to have spin and parity of $7/2^-$, $9/2^-$ or $11/2^-$. The $9/2^-$ and $11/2^-$ assignments can be excluded, since only an $M2$ transition with $E_\gamma =$ 429 keV from the $13/2^+$ isomeric state to the $9/2^-$ ground state was observed in ^{191}Bi [33,34]. If the spin value of the 148.7(5) keV excited state had been 9/2 or higher, at least a weak transition from the $13/2^+$ state to the excited state with a multipolarity of $M2$ or lower should have been observed.

The unhindered alpha-decay of ^{195}At to the $7/2^-$ state at 148.7(5) keV in ^{191}Bi with a hindrance factor of 1.17(6), indicates that the alpha-decay originates from a state with the same $7/2^-$ assignment in ^{195}At. Taking into account the 242 keV [30] excitation energy of the $1/2^+$ state in ^{191}Bi and the observed alpha-decay energies of ^{195}At, it was concluded that the $1/2^+$ state becomes the ground state in ^{195}At and the $7/2^-$ state lies at an excitation energy of 32(7) keV.

The expectation value for the number of correlated triple chains of the type $\mathrm{ER} - \alpha_\mathrm{m} - \alpha_\mathrm{d}$ produced by random correlations between both correlation pairs in the energy region of 7000 keV–7300 keV for the mother and 6250 keV–6350 keV for the daughter alpha-decay was estimated to be 2.9. The number of random correlations between the found $\mathrm{ER} - \alpha_\mathrm{m}$ correlation pairs and candidate daughter alpha-decays was estimated to be 59 (see table 2). The estimates of random correlations were determined according to ref. [22].

3.3 Decay of the $1/2^+$ state in ^{191}Bi

An alpha-decay energy of $E_\alpha = 6963(4)$ keV and a half-life $T_{1/2} = (341^{+50}_{-40})$ ms were determined for the mother alpha activity and $E_\alpha = 6313(4)$ keV and $T_{1/2} = 16(3)$ s for the daughter alpha activity from the 63 $\mathrm{ER} - \alpha_\mathrm{m} - \alpha_\mathrm{d}$ correlated decay chains of group C shown in figs. 2 and 3a. The search times used for $\mathrm{ER} - \alpha_\mathrm{m}$ and $\alpha_\mathrm{m} - \alpha_\mathrm{d}$ correlation pairs were 4 s and 80 s, respectively.

In group C, the properties of the mother activity are compatible with the alpha-decay of the $1/2^+$ state in ^{195}At to the $1/2^+$ state in ^{191}Bi, but the daughter activity has the properties consistent with the alpha-decay of the $9/2^-$ state in ^{191}Bi. The unobserved link between the $1/2^+$ and $9/2^-$ states in ^{191}Bi can be explained by an $E3$ transition from the $1/2^+$ state to the excited $7/2^-$ state followed by an $M1$ transition from that state to the $9/2^-$ ground state. The proposed decay scheme of the $1/2^+$ state in ^{191}Bi is presented in fig. 6.

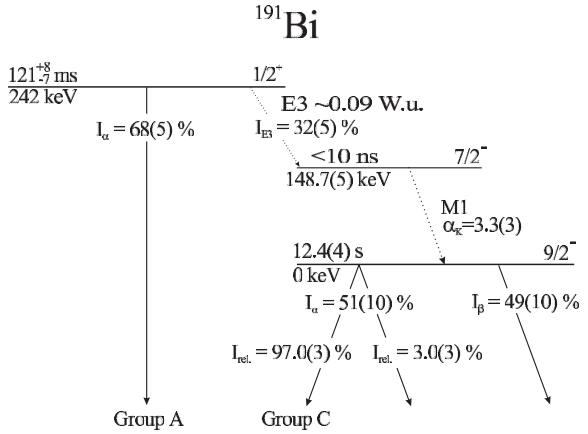

Fig. 6. Proposed decay scheme of the $1/2^+$ state in ^{191}Bi. The branching ratios of the alpha-decay and the $E3$ transition of the $1/2^+$ state were estimated from the numbers of $\mathrm{ER} - \alpha_\mathrm{m} - \alpha_\mathrm{d}$ correlated decay chains in groups A and C shown in fig. 2. The linking transitions between $1/2^+$ and $9/2^-$ states were not directly observed, but the $M1$ transition was observed to follow the alpha-decay of the $7/2^-$ state in ^{195}At. The absolute alpha-decay branching ratio of the $9/2^-$ state was estimated using the number of $\mathrm{ER} - \alpha_\mathrm{m}$ and $\mathrm{ER} - \alpha_\mathrm{m} - \alpha_\mathrm{d}$ correlated decay chains where the mother alpha-decay from the $7/2^-$ state in ^{195}At to the $7/2^-$ state in ^{191}Bi was observed in coincidence with gamma- or X-ray events originating from the $M1$ transition. The relative alpha-decay branching ratios of the $9/2^-$ state were taken from refs. [13,30]. See text and fig. 7 below for more details.

If an absolute branching ratio of 51(10)% for the alpha-decay of the $9/2^-$ ground state in ^{191}Bi is assumed, branching ratios of 32(5)% and 68(5)% are obtained for the $E3$ transition and the alpha-decay from the $1/2^+$ excited state in ^{191}Bi, respectively. These branching ratios were estimated from the numbers of the $\mathrm{ER} - \alpha_\mathrm{m} - \alpha_\mathrm{d}$ correlated decay chains in groups A and C in fig. 2. The obtained branching ratio of 68(5)% for the alpha-decay is in agreement with the previously reported values (50–100)% [13] and (85^{+15}_{-35})% [3]. The partial half-life of the 93(7) keV $E3$ transition from the 242 keV excited $1/2^+$ state to the 148.7(5) keV excited $7/2^-$ state in ^{191}Bi is approximately 380 ms when a branching ratio of 32(5)% is assumed. The Weisskopf estimate for a 93 keV $E3$ transition in bismuth corrected for internal conversion taken from ref. [31] is approximately 34 ms. Thus, the strength

The number of accidentally correlated triple chains in the region of group C in fig. 2 was estimated to be 0.8. The expectation value for the number of accidental correlations between the found $\mathrm{ER} - \alpha_\mathrm{m}$ correlation pairs and the candidate daughter alpha-decays in the same region was estimated to be 17 (see table 2).

Table 3. The measured alpha-decay properties of ^{195}At and the daughter nucleus ^{191}Bi. The literature values for the alpha-decay energy and half-life of ^{195}At are taken from ref. [10]. The literature values and assignments for ^{191}Bi are taken from ref. [13]. The alpha-decay hindrance factors HF and reduced widths δ^2 are calculated from measured values (except for the 6639(5) keV alpha-decay in ^{191g}Bi) using the method of Rasmussen [28] and normalised to the alpha-decay of ^{212}Po. In the calculation, the $\Delta\ell$ values of the transitions were taken into account. The identification of 6639(5) keV alpha-decay from the ground state of ^{191}Bi was not attempted (see sect. 4 for more details).

Nucleus	E_α (keV)		$T_{1/2}$ (ms)		$I_{\mathrm{rel.}}$(%)		HF	δ^2(keV)	$\Delta\ell$	Assignment
	This work	Lit.	This work	Lit.	This work	Lit.				
^{195g}At	6953(3)	6960(20)	328(20)	385^{+69}_{-51}	100		0.92(7)	70(5)	0	$1/2^+ \rightarrow 1/2^+$
^{195m}At	7075(4)		147(5)		95.5(5)		1.17(6)	55(3)	0	$7/2^- \rightarrow 7/2^-$
^{195m}At	7221(4)		147(5)		4.5(5)		47(6)	1.4(2)	2	$7/2^- \rightarrow 9/2^-$
^{191g}Bi[(a)]	6308(3)	6311(5)	12.4(4) s	12(1) s		100	1.5(4)	42(9)	0	$9/2^- \rightarrow 9/2^-$
^{191g}Bi		6639(5)		12(1) s		3.0(3)	68(28)	0.9(4)	5	$9/2^- \rightarrow 1/2^+$
^{191m}Bi[(b)]	6870(3)	6876(5)	121^{+8}_{-7}	150(15)	100		1.5(2)	43(5)	0	$1/2^+ \rightarrow 1/2^+$

([a]) Measured absolute $I_\alpha = 51(10)$%. Literature value $I_\alpha = 40$–77%.
([b]) Measured absolute $I_\alpha = 68(5)$% and $I_{E3} = 32(5)$%. Literature value $I_\alpha = 50$–100%.

of the inferred $E3$ transition between the $1/2^+$ and the $7/2^-$ states is approximately 0.09 W.u.

4 Discussion

The alpha-decay properties of ^{195}At and ^{191}Bi observed in the present work are summarised in table 3. The results are compared with the previous values taken from refs. [10] and [13]. In the present work, the identification of the 3% alpha-decay branch from the $9/2^-$ ground state in ^{191}Bi to the $1/2^+$ ground state in ^{187}Tl [13,30] was not attempted. The reason for this was that the alpha-decay energy of this branch (6639(5) keV [13]) would appear in the ER$-\alpha_{\mathrm{m}}-\alpha_{\mathrm{d}}$ correlated events in the region where a large number of accidentally correlated decay chains could also be expected (see fig. 2).

The alpha-decay hindrance factors HF and reduced widths δ^2 are calculated according to the method of Rasmussen [28] and normalised to the alpha-decay of ^{212}Po.

Based on the results of the present work and ref. [13], the decay schemes of ^{195}At and ^{191}Bi are constructed and shown in fig. 7. For comparison the decay schemes of ^{197}At [15] and ^{193}Bi [13] are also presented. As explained in the previous section, the $1/2^+$ intruder state, having a $\pi(4p{-}1h)$ configuration, was determined to be the ground state in ^{195}At. This was already speculated by Coenen *et al.* in ref. [15], due to the low 52(10) keV excitation energy of this state in ^{197}At. This is indeed observed in the present work. A more dramatic observation, however, was that the $9/2^-$ state with $(\pi h_{9/2})^3$ configuration, which is the ground state in all heavier odd-mass astatine isotopes from ^{197}At to ^{211}At, was not observed in ^{195}At. Instead of the $9/2^-$ state a $7/2^-$ state was observed as the first-excited state with an excitation energy of 32(7) keV.

Based on the Nilsson diagram, the emergence of the $7/2^-$ state over the $9/2^-$ state can be understood by assuming a change in the quadrupole deformation of this three-particle configuration between ^{197}At and ^{195}At. As discussed in ref. [35], no sizeable ground-state deformation was observed in ^{197}At, thus the last proton in the $\pi h_{9/2}$ orbital creates the $9/2^-$ ground state. If sufficient oblate deformation is assumed in ^{195}At, the $7/2^-$ state associated with a $7/2^-[514]$ Nilsson state, originated predominantly from the $\pi h_{9/2}$ orbital at sphericity and having a mixed $\pi f_{7/2}/\pi h_{9/2}$ character at oblate deformations, becomes available for the 85th proton. A similar dramatic change in the ground-state deformation from $\beta_2 = 0.08$ to $\beta_2 = -0.21$ was theoretically predicted to occur between ^{199}At and ^{198}At by Möller *et al.* [36]. Based on the results obtained in the present work, it is proposed that the deformed three-particle configuration, driving the last proton to the $7/2^-[514]$ Nilsson state, becomes energetically more favoured than the near-spherical $(\pi h_{9/2})^3$ configuration when moving from ^{197}At to ^{195}At. The existence of a low-lying $7/2^-$ state in ^{191}Bi can be similarly explained by the $7/2^-[514]$ Nilsson state, which is actually the only conceivable state where the low-lying $7/2^-$ level would originate in bismuth isotopes.

The alpha-decay of the $7/2^-$ state in ^{195}At can be thought to occur most simply by removing a proton pair from the $\pi h_{9/2}$ orbital. The remaining proton in the $7/2^-[514]$ Nilsson state represents the 148.7(5) keV excited state in ^{191}Bi, which was observed to decay via an $M1$ transition to the $9/2^-$ ground state. The alpha-decay between the $7/2^-$ states represents an unhindered process, which is in good agreement with the observed hindrance factor of 1.17(6) presented in table 3. This unhindered alpha-decay was used to determine the spin and parity of the decaying state in ^{195}At, after the spin and parity of the final state in ^{191}Bi were determined as discussed in sect. 3.2. The alpha-decay from the $7/2^-$ state directly to the $9/2^-$ ground state in ^{191}Bi would require the rearrangement of the proton configuration. This manyfold process with $\Delta\ell = 2$, would represent a hindered alpha-decay. The

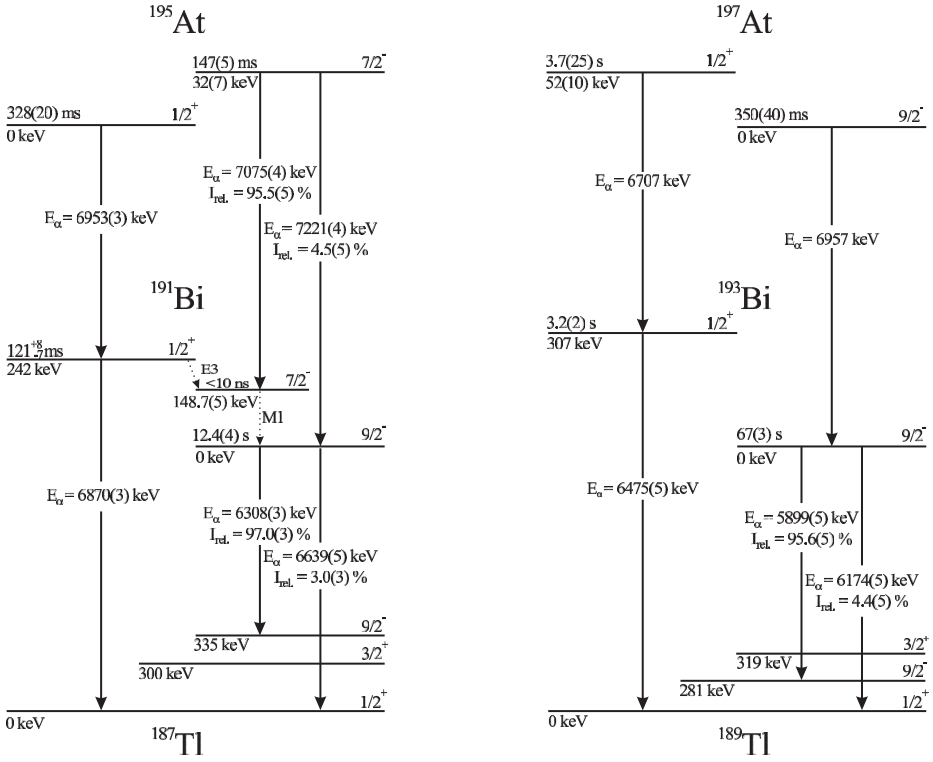

Fig. 7. The decay properties and low-lying levels in ^{195}At and ^{197}At and in the corresponding daughter nuclei ^{191}Bi and ^{193}Bi. The data are taken from the present work and from refs. [13,15] (see also fig. 6).

obtained alpha-decay hindrance factor of 47(6) is consistent with this assumption (see table 3).

The $13/2^+$ state, which is observed in ^{197}At [35] and ^{193}At [37] was not found in ^{195}At in the present work. The decay mode of this state would give additional information about the characteristics of the $7/2^-$ state in ^{195}At.

In ^{197}At the $13/2^+$ state was observed to decay via an $M2$ gamma-ray transition to the $9/2^-$ ground state having a gamma-ray energy of $E_\gamma = 310.7(1)$ keV and lifetime of $\tau = 8(2)$ μs [35]. The corresponding $M2$ transition was not observed in ^{193}At, but the $13/2^+$ state was observed to alpha-decay to the corresponding $13/2^+$ state in ^{189}Bi. The possible electromagnetic transition from the $13/2^+$ state in ^{193}At, corresponding to the $M2$ transition in ^{197}At, was deduced to be of $E3$ character [37] decaying not to a $9/2^-$ state, but to a $7/2^-$ state. A similar $E3$ transition can also be expected to occur in ^{195}At. By determining the strength of the possible $E3$ transition from the $\pi i_{13/2}$ orbital, it would be possible to estimate the character or even mixing of the final state consisting of the $\pi h_{9/2}$ and $\pi f_{7/2}$ orbitals as explained in refs. [38,39].

The existence of the low-lying $7/2^-$ state in ^{191}Bi allows the possibility of an $E3$ transition from the $1/2^+$ state as shown in fig. 6. The transition was not observed directly, but the correlated decay chains of group C in fig. 2 require linking transitions between the $1/2^+$ and $9/2^-$ states in ^{191}Bi, as discussed in sect. 3.2. The deduced $E3$ transition strength of 0.09 W.u. is a typical value for transitions related to a change of the single-particle orbital in this region of the nuclear chart.

The absolute alpha-decay branching ratio of the $9/2^-$ ground state in ^{191}Bi was measured to be 51(10)%. The remaining 49(10)% of the decay is assumed to occur through beta-decay, giving a partial beta-decay half-life of approximately 25 s. This value is consistent with the theoretical prediction of 17.5 s given for the ground-state beta-decay half-life of ^{191}Bi in ref. [40]. The corresponding theoretical estimate for the beta-decay half-life of the ^{195}At ground state is 4.2 s, which is much longer than the measured half-life. The beta-decay branching ratio for ^{195}At could not be measured in the present experiment.

Tagaya *et al.* [10] reported that they had measured two alpha-decaying levels in ^{195}At. The alpha-decay assigned to proceed from the $(1/2^+)$ state (see table 3) is in good agreement with the result obtained in the present work. The half-life of the other state is also consistent with our result, but due to lower statistics the complicated fine structure of the alpha-decay was not observed in the work of Tagaya *et al.*. Therefore, the energy of the alpha-decay $E_\alpha = 7105(30)$ keV directly to the ^{191}Bi ground state deduced in their work [10] is approximately 115 keV lower than the corresponding alpha-decay energy observed in the present work. Due to this difference Tagaya *et al.* achieved different ordering of the high-spin and low-spin states in ^{195}At than proposed in the present work and previously in ref. [5] (see fig. 7).

A mass excess of $-3500(90)$ keV was evaluated for the ground state of ^{195}At using the measured nuclear masses linked by alpha-decay chains in ref. [41]. In that work the decay properties presented in fig. 7 were used

for the ground-state decay of ^{195}At. Using the mass excess of $-11030(90)$ keV reported for ^{194}Po in ref. [41], the proton separation energy of ^{195}At was calculated to be $S_p = -240(130)$ keV. This indicates that the proton drip line has already been crossed. The branching ratio for the proton decay, however, is prohibitively small for observation. The first realistic candidate to observe the proton decay from the ground state in the astatine isotopes would be ^{189}At [37].

In the present work, the maximum production cross-section of ^{195}At (including the $1/2^+$ and $7/2^-$ states) was determined to be $\sigma \sim 200$ nb at the bombarding energy of $E = 262$ MeV in the middle of the target for the reaction ^{142}Nd(^{56}Fe,p2n)^{195}At. The production ratios of the $1/2^+$ ground state and the $7/2^-$ isomeric state were approximately 14% and 86%, respectively. When this isotope was produced in the reaction ^{141}Pr(^{56}Fe,2n)^{195}At [5], at the bombarding energy of $E = 230$ MeV a total production cross-section of $\sigma \sim 900$ nb was determined (here a transmission of 40% for evaporation residues is assumed). The excitation function of the 2n-channel was partially cut by the Coulomb barrier. For the 3n-channel of the reaction ^{141}Pr(^{56}Fe,3n)^{194}At [5], the maximum production cross-section at a bombarding energy of $E = 248$ MeV was measured to be $\sigma \sim 1.5$ μb.

The experiment discussed in the present work was dedicated to produce new radon isotopes [19], and the astatine isotopes were produced as side-products. From the production cross-sections given above, it can be quite clearly seen that in this region of the nuclear chart it is more favourable to produce very neutron-deficient isotopes by evaporation of neutrons.

5 Conclusion

The alpha-decay properties of ^{195}At were studied with improved accuracy. The $1/2^+$ intruder state was determined as the ground state and the $7/2^-$ state was observed as the first-excited state. The $9/2^-$ state, which is the ground state in the heavier odd-mass astatine isotopes from ^{197}At to ^{211}At, was not observed. These dramatic changes between ^{197}At and ^{195}At were concluded to indicate different shapes of the $9/2^-$ and the $7/2^-$ states of the isotopes. A new low-lying excited state in ^{191}Bi with spin and parity of $7/2^-$ was observed via alpha-decay. The character of the new state was determined from the properties of an observed gamma-ray transition. The same spin and parity of $7/2^-$ were deduced for the initial state in ^{195}At based on the observation of an unhindered alpha-decay to the $7/2^-$ state in the daughter nucleus ^{191}Bi.

This work was supported by the Academy of Finland under the Finnish Centre of Excellence Programme 2002-2005 (Project No. 44875, Nuclear and Condensed Matter Physics Programme at JYFL).

References

1. W. Treytl, K. Valli, Nucl. Phys. A **97**, 405 (1967).
2. S. Yashita, Thesis, Lawrence Radiation Laboratory, Berkeley, 1983, unpublished.
3. M. Leino, Thesis, University of Helsinki Report Series in Physics, HU-P-D37/1983, unpublished.
4. A. Ghiorso, S. Yashita, M. Leino, L. Frank, J. Kalnins, P. Armbruster, J.-P. Dufour, P.K. Lemmertz, Nucl. Instrum. Methods A **269**, 192 (1988).
5. T. Enqvist, Thesis, Department of Physics, University of Jyväskylä, Research Report No. 3/1996, unpublished.
6. M. Leino, J. Äystö, T. Enqvist, P. Heikkinen, A. Jokinen, M. Nurmia, A. Ostrowski, W.H. Trzaska, J. Uusitalo, P. Armbruster, V. Ninov, Nucl. Instrum. Methods B **99**, 653 (1995).
7. M. Leino, J. Äystö, T. Enqvist, A. Jokinen, M. Nurmia, A. Ostrowski, W.H. Trzaska, J. Uusitalo, K. Eskola, P. Armbruster, V. Ninov, Acta Phys. Pol. B **26**, 309 (1995).
8. D. Seweryniak, J. Uusitalo, C.R. Bingham, W. Reviol, X.-J. Xu, J.C. Batchelder, K.S. Toth, J.L. Wood, J.A. Cizewski, ANL-98/24 (Physics Division Ann. Rep., 1997) (1998) 16.
9. C.N. Davids, B.B. Back, K. Bindra, D.J. Henderson, W. Kutschera, T. Lauritsen, Y. Nagame, P. Sugathan, A.V. Ramayya, W.B. Walters, Nucl. Instrum. Methods B **70**, 358 (1992).
10. Y. Tagaya, S. Hashimoto, K. Morita, Y.H. Pu, T. Ariga, K. Ohta, T. Minemura, I. Hisanaga, T. Motobayashi, T. Nomura, Eur. Phys. J. A **5**, 123 (1999).
11. H. Miyatake, T. Nomura, H. Kawakami, J. Tanaka, M. Oyaizu, K. Morita, T. Shinozuka, H. Kudo, K. Sueki, Y. Iwata, Nucl. Instrum. Methods B **26**, 309 (1987).
12. K. Heyde, P. Van Isacker, M. Waroquier, J.L. Wood, R.A. Meyer, Phys. Rep. **102**, 291 (1983).
13. E. Coenen, K. Deneffe, M. Huyse, P. Van Duppen, J.L. Wood, Phys. Rev. Lett. **54**, 1783 (1985).
14. J.C. Batchelder, K.S. Toth, C.R. Bingham, L.T. Brown, L.F. Conticchio, C.N. Davids, R.J. Irvine, D. Seweryniak, W.B. Walters, J. Wauters, E.F. Zganjar, J.L. Wood, C. DeCoster, B. Decroix, K. Heyde, Eur. Phys. J. A **5**, 49 (1999).
15. E. Coenen, K. Deneffe, M. Huyse, P. Van Duppen, J.L. Wood, Z. Phys. A **324**, 485 (1986).
16. R.G. Allatt, R.D. Page, M. Leino, T. Enqvist, K. Eskola, P.T. Greenlees, P. Jones, R. Julin, P. Kuusiniemi, W.H. Trzaska, J. Uusitalo, Phys. Lett. B **437**, 29 (1998).
17. C.N. Davids, P.J. Woods, H.T. Penttilä, J.C. Batchelder, C.R. Bingham, D.J. Blumenthal, L.T. Brown, B.C. Busse, L.F. Conticchio, T. Davinson, D.J. Henderson, R.J. Irvine, D. Seweryniak, K.S. Toth, W.B. Walters, B.E. Zimmerman, Phys. Rev. Lett. **76**, 592 (1996).
18. G.L. Poli, C.N. Davids, P.J. Woods, D. Seweryniak, M.P. Carpenter, J.A. Cizewski, T. Davinson, A. Heinz, R.V.F. Janssens, C.J. Lister, J.J. Ressler, A.A. Sonzogni, J. Uusitalo, W.B. Walters, Phys. Rev. C **63**, 044304 (2001).
19. H. Kettunen, J. Uusitalo, M. Leino, P. Jones, K. Eskola, P.T. Greenlees, K. Helariutta, R. Julin, S. Juutinen, H. Kankaanpää, P. Kuusiniemi, M. Muikku, P. Nieminen, P. Rahkila, Phys. Rev. C **63**, 044315 (2001).
20. H. Koivisto, J. Ärje, N. Nurmia, Nucl. Instrum. Methods B **94**, 291 (1994).

21. J.F. Ziegler, J.P. Biersack, U. Littmark, *The Stopping and Range of Ions in Solids* (Pergamon, New York, 1985).
22. K.-H. Schmidt, C.-C. Sahm, K. Pielenz, H.-G. Clerc, Z. Phys. A **316**, 19 (1984).
23. K.-H. Schmidt, Eur. Phys. J. A **8**, 141 (2000).
24. R.D. Page, P.J. Woods, R.A. Cunningham, T. Davinson, N.J. Davis, A.N. James, K. Livingston, P.J. Sellin, A.C. Shotter, Phys. Rev. C **53**, 660 (1996).
25. J. Wauters, P. Dendooven, M. Huyse, G. Reusen, P. Van Duppen, P. Lievens and the ISOLDE Collaboration, Phys. Rev. C **47**, 1447 (1993).
26. A. Rytz, At. Data Nucl. Data Tables **47**, 205 (1991).
27. Y.H. Pu, K. Morita, M.G. Hies, K.O. Lee, A. Yoshida, T. Nomura, Y. Tagaya, T. Motobayashi, M. Kurokawa, H. Minemura, T. Uchibori, T. Ariga, K. Sueki, S.A. Shin, Z. Phys. A **357**, 1 (1997).
28. J.O. Rasmussen, Phys. Rev. **113**, 1593 (1959).
29. P. Van Duppen, P. Decrock, P. Dendooven, M. Huyse, G. Reusen, J. Wauters, Nucl. Phys. A **529**, 268 (1991).
30. R.B. Firestone, V.S. Shirley, *Table of Isotopes*, 8th edition (Wiley, New York, 1996).
31. J. Kantele, *Handbook of Nuclear Spectrometry*, (Academic Press, London, 1995).
32. P.A. Butler, private communication.
33. P. Nieminen, J.F.C. Cocks, O. Dorvaux, P.T. Greenlees, K. Helariutta, P.M. Jones, R. Julin, S. Juutinen, H. Kankaanpää, H. Kettunen, P. Kuusiniemi, M. Leino, M. Muikku, P. Rahkila, A. Savelius, J. Uusitalo, A.N. Andreyev, F. Becker, K. Eskola, K. Hauschild, M. Houry, M. Huyse, W. Korten, Y. Le Coz, R. Lucas, T. Lönnroth, Ch. Theisen, K. Van de Vel, P. Van Duppen, N. Amzal, P.A. Butler, N. Hammond, C. Scholey, R. Wyss, Acta Phys. Pol. B **32**, 1019 (2001).
34. A.N. Andreyev, D. Ackermann, P. Cagarda, J. Gerl, F.P. Heßberger, S. Hofmann, M. Huyse, A. Keenan, H. Kettunen, A. Kleinböhl, A. Lavrentiev, M. Leino, B. Lommel, M. Matos, G. Münzenberg, C.J. Moore, C.D. O'Leary, R.D. Page, S. Reshitko, S. Saro, C. Schlegel, H. Schaffner, M.J. Taylor, P. Van Duppen, L. Weissman, R. Wyss, Eur. Phys. J. A **10**, 129 (2001).
35. M.B. Smith, R. Chapman, J.F.C. Cocks, O. Dorvaux, K. Helariutta, P. Jones, R. Julin, S. Juutinen, H. Kankaanpää, H. Kettunen, P. Kuusiniemi, Y. Le Coz, M. Leino, D.J. Middleton, M. Muikku, P. Nieminen, P. Rahkila, A. Savelius, K.-M. Spohr, Eur. Phys. J. A **5**, 43 (1999).
36. P. Möller, J.R. Nix, W.D. Myers, W.J. Swiatecki, At. Data Nucl. Data Tables **59**, 185 (1995).
37. H. Kettunen, T. Enqvist, T. Grahn, P.T. Greenlees, P. Jones, R. Julin, S. Juutinen, A. Keenan, P. Kuusiniemi, M. Leino, A.-P. Leppänen, P. Nieminen, J. Pakarinen, P. Rahkila, J. Uusitalo, submitted to Eur. Phys. J. A.
38. I. Bergström, B. Fant, Phys. Scr. **31**, 26 (1985).
39. G.D. Dracoulis, T. Kibédi, A.P. Byrne, A.M. Baxter, S.M. Mullins, R.A. Bark, Phys. Rev. C **63**, 061302 (2001).
40. P. Möller, J.R. Nix, K.-L. Kratz, At. Data Nucl. Data Tables **66**, 131 (1997).
41. Yu.N. Novikov, F. Attallah, F. Bosch, M. Falch, H. Geissel, M. Hausmann, Th. Kerscher, O. Klepper, H.-J. Kluge, C. Kozhuharov, Yu.A. Litvinov, K.E.G. Löbner, G. Münzenberg, Z. Patyk, T. Radon, C. Scheidenberger, A.H. Wapstra, H. Wollnik, Nucl. Phys. A **697**, 92 (2002).